CHAPTER 4

RAY CURVATURE AND REFRACTION OF WAVE PACKETS

by

J. Ernest Breeding, Jr.

Department of Oceanography and Ocean Engineering
Florida Institute of Technology
Melbourne, Florida 32901

ABSTRACT

Directional wave data obtained simultaneously at two measurement sites is used to confirm the constancy, and therefore the validity, of Snell's laws for wave packets. It is found that the wave packets refract according to Snell's law with the geometric group velocity whereas the wavelets within a packet refract according to Snell's law with phase velocity.

An expression for the ray curvature of a wave packet is derived which is suitable for use in wave prediction programs. The ray curvature of the wave packet is found to vanish if the packet direction becomes either perpendicular or parallel to the wave speed contours, assuming the wavelet direction is not parallel to the contours. This means that as a hydron (wave packet) moves into shoaling water refraction tends eventually to turn the hydron so that it is directed either perpendicular or parallel to the shoreline. The first case is similar to monochromatic waves. For parallel water depth contours, it is the result for hydrons which begin in deep water if the angle of incidence is between 0^0 and 74.8^0 with respect to the contour normal. However, for deep water angles of incidence equal to or greater than 74.8^0 the hydrons are turned and move parallel to shore in water of intermediate depth. The packet ray curvature approaches infinity as the wavelet direction, but not the hydron direction, becomes parallel to the wave speed contours. The result is total reflection of the waves. Total reflection occurs if a hydron is moving into deeper water and its initial direction exceeds a critical angle. At the reflection point the hydron direction becomes perpendicular to the water depth contours. Further, the hydron velocity goes to zero, which is consistent with a particle concept. As in quantum mechanics, the wave-particle duality is encountered.

1 INTRODUCTION

The conventional definition of group speed U has been defined as

$$U = d\omega/dk \tag{1}$$

where ω is the angular frequency and k is the wave number. This equation defines the speed of the group in the direction of the wavelet velocity. The geometric group speed G was defined by Breeding (1978a) as

$$G = U \cos \phi \tag{2}$$

where

$$\phi = \theta - \gamma \tag{3}$$

The direction of movement of the wave packet is represented by θ, and the direction the wavelets move within the packet is specified by γ.

Breeding (1978a) and Black (1979) have found that the trajectories of wave packets are not determined by a monochromatic refraction law, i.e., by simply using Snell's law with phase velocity. Based on a comparison of computed backtracks from the measurement site with the known source of the waves, Breeding (1978a) has shown that wave packets refract according to Snell's law with the geometric group velocity. This refraction law determines the wave path of constructive interference. At each point of the wave packet trajectory the wavelet direction is determined by Snell's law with phase velocity.

One objective of this paper is to investigate more directly the validity of the refraction laws by testing the constancy of Snell's laws for the wave packets and wavelets using directional wave data obtained simultaneously at two measurement sites. A further purpose of the paper is to derive an expression for the ray curvature of a wave packet which is suitable for use in wave prediction programs. Properties of the packet ray curvature are described, and the important features of wave packet refraction are demonstrated using examples of gravity water waves.

2 TEST OF WAVE PACKET REFRACTION LAWS

2.1 Theory

Snell's law for a wave packet can be stated

$$(\sin \theta)/G = C_G \tag{4}$$

where C_G is a constant for a given frequency. The direction of γ is determined by

$$(\sin \gamma)/v = C_v \tag{5}$$

which is Snell's law with phase velocity where $v = \omega/k$ is the phase speed and C_v is a constant for a given frequency. To use (4) and (5) the y-axis is taken parallel with the wave speed contours. By virtue of Snell's law with phase velocity, γ is a function of k. The water depth h is assumed to vary slowly over the distance of a wavelength so that k is given by the classical dispersion relation

$$\omega^2 = gk \tanh kh \tag{6}$$

where g is the acceleration due to gravity. By considering the variation of (5) with respect to frequency it is found that (Breeding, 1978a)

$$\tan \phi = k(d\gamma/dk) \tag{7}$$

which is a useful relation for determining θ from a set of wave measurements.

2.2 Field Observations

2.2.1 Directional wave data

Hurricane Betsy passed over the southern tip of Florida and entered the Gulf of Mexico at about 1500 UT on September 8, 1965. After making a curved path the hurricane entered land at the Mississippi Delta at about 0400 UT on September 10. The storm had winds in excess of 100 knots.

Waves due to Hurricane Betsy were measured (Breeding, 1972) using two independent arrays of six pressure transducers which were placed on the sea floor at the sites of two offshore platforms (stages) near Panama City, Florida. The location and configuration of the arrays are shown in Figure 1. In each array a pressure sensor is located at each corner of a pentagon of side 35.8 m (117.6 ft) and these sensors are located 30.5 m (100.0 ft) from a sensor at the center of the array. Stage 1 is located in 31.7 m (104 ft) of water 17.7 km (11 mi) from shore. Stage 2 is located in 19.2 m (63 ft) of water 2.8 km (1.7 mi) from shore. Directional power spectra with 60 d.f. were computed for time series records about 30 min in length by Bennett (1972) based on the method of Munk et al. (1963).

The results of the wave directional analysis for successive measurement times of 1712 - 1743 and 1744 - 1815 UT on September 9, 1965 at Stage 1 are shown in Figure 2. In the array pressure sensors 1, 2, 4, and 5 were operational. The wavelet directions shown are the bearings from which the waves come relative to true north. It is apparent that the findings for the two measurement periods are consistent. The wave directional results for measurements made independently at Stage 2 for the same times as presented for Stage 1 are shown in Figure 3. For this array all the sensors were working but sensors 2 and 4.

2.2.2 Test of Snell's laws

For the observations presented in Figures 2 and 3 the wavelet direction γ and an estimate of the slope $d\gamma/dk$ were obtained by fitting a quadratic polynomial to the data by the method of least squares. The resulting quadratic curves are shown with the data in the figures. The polynomial obtained for the Stage 1 data is given by

$$\gamma_1 = 3.724 - 17.26\, k_1 + 68.32\, k_1^2 \tag{8}$$

The similar finding for the Stage 2 data is

$$\gamma_2 = 3.984 - 18.74\, k_2 + 92.06\, k_2^2 \tag{9}$$

Once γ and $d\gamma/dk$ are determined for a given wavelet period from (8) and (9), the wave packet bearings can be determined for each measurement site, respectively, using (7) and (3). For example, for a wavelet period

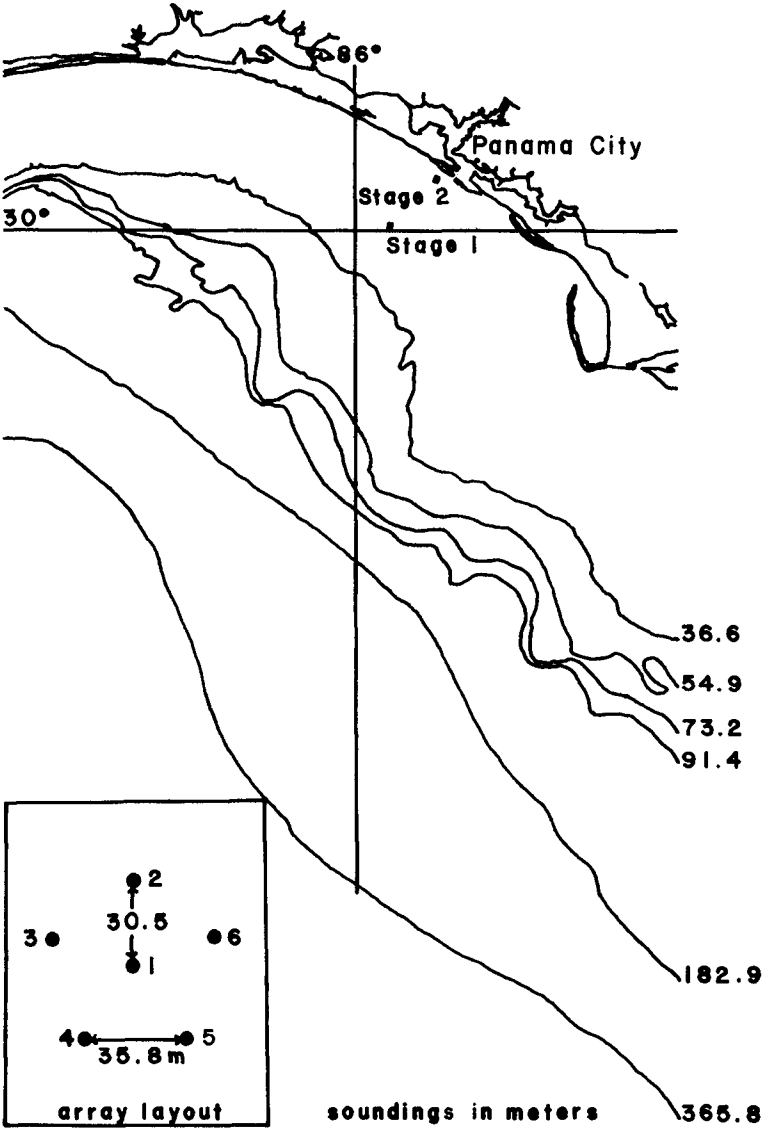

Figure 1. Bottom topography and array configuration near Panama City, Florida.

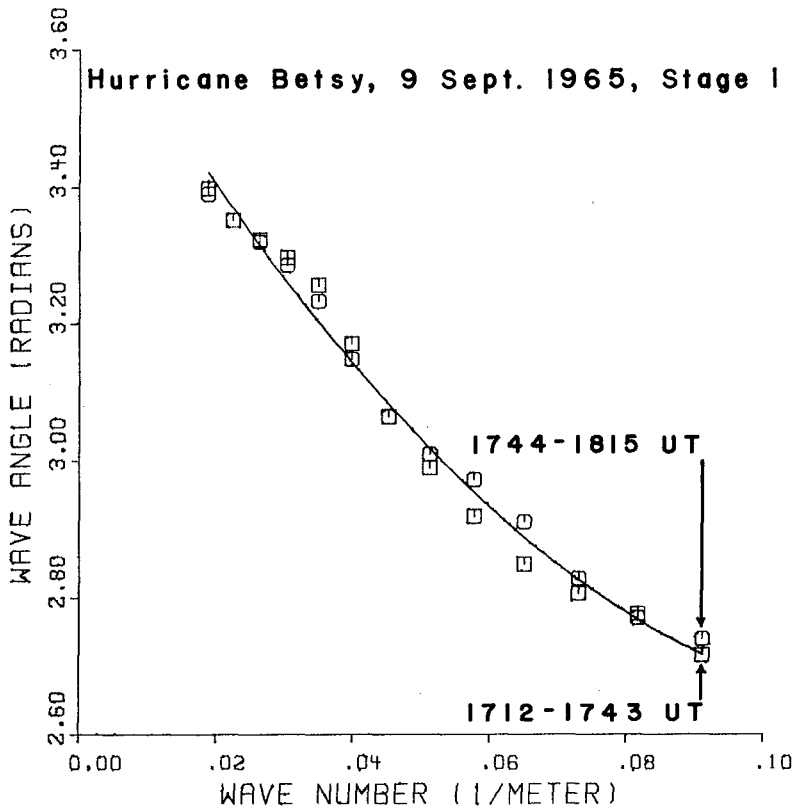

Figure 2. Wavelet directions as a function of wave number at Stage I.

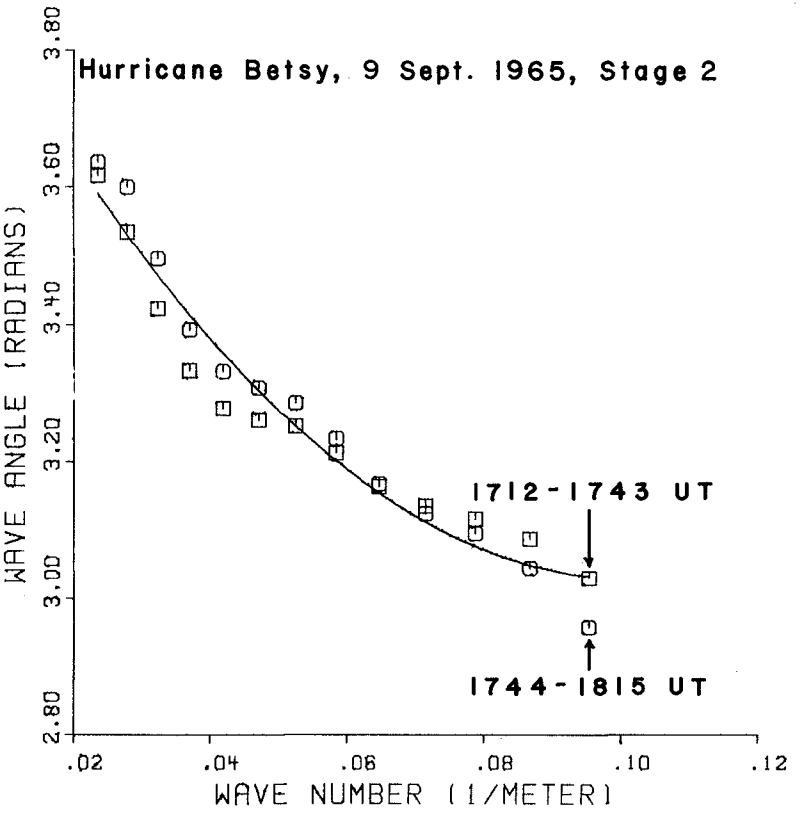

Figure 3. Wavelet directions as a function of wave number at Stage 2.

of 10.9 s, at Stage 1 $v_1 = 14.48$ m/s, $\gamma_1 = 180.19^0$, $G_1 = 9.23$ m/s, and $\theta_1 = 154.97^0$. The corresponding values at Stage 2 are $v_2 = 12.23$ m/s, $\gamma_2 = 189.37^0$, $G_2 = 8.89$ m/s, and $\theta_2 = 164.01^0$.

To evaluate the constants in Snell's laws the wave packet and wavelet directions are defined with respect to the normal to the water depth contours. The water depth contours between the stages are approximately parallel with a bearing of 131^0 with respect to true north. For the data summarized by (8) and (9) the Snell's law constants for both the wave packets and wavelets were evaluated for each wavelet period. The percentage differences of the constants at Stage 2 from the corresponding values at Stage 1 are shown in Figure 4. In the same figure the surface extrapolations of the energy density for the first of the two measurement periods used to determine (8) and (9) are presented for both stages.

2.2.3 Discussion of the results

The difference in the energy density for Stage 1 and Stage 2 shown in Figure 4 is a manifestation of the wave modification occurring between the stages. Over most of the frequency range considered, the Snell's law constants at Stage 2 differ by less than ±10% from the corresponding constants at Stage 1 for both the wave packets and the wavelets. The difference in the constants increases as the waves become less energetic. However, the difference in the constants is less than 5% for both the wave packets and the wavelets at the wave period where the energy density peaks. These findings are significant. Although the validity of Snell's law with phase velocity is well established, the results presented here indicate that Snell's law with the geometric group velocity is equally valid.

There are a number of reasons why different constants are found for Snell's laws for the wave packets and wavelets at the offshore stages. For example, a measurement error of a few degrees for each array is possible from inaccuracies in locating the positions of the pressure sensors. The water depth contours are not exactly parallel as was assumed in the computations. Further, the accuracy in determining the Snell's law constants for the wave packets depends upon the method used in evaluating the slope $d\gamma/dk$ from the data. Higher accuracy could be achieved by the use of higher order polynomials to better fit the data.

3 RAY CURVATURE FOR WAVE PACKETS

It is more convenient tc determine ray trajectories using the ray curvature than it is to use Snell's law. The ray curvature κ_v of a ray moving with phase speed v was derived by Munk and Arthur (1952) and Arthur, et al (1952) as

$$\kappa_v = \frac{d\gamma}{ds_v} = \frac{1}{v} \left(\sin \gamma \frac{\partial v}{\partial x} - \cos \gamma \frac{\partial v}{\partial y} \right) \qquad (10)$$

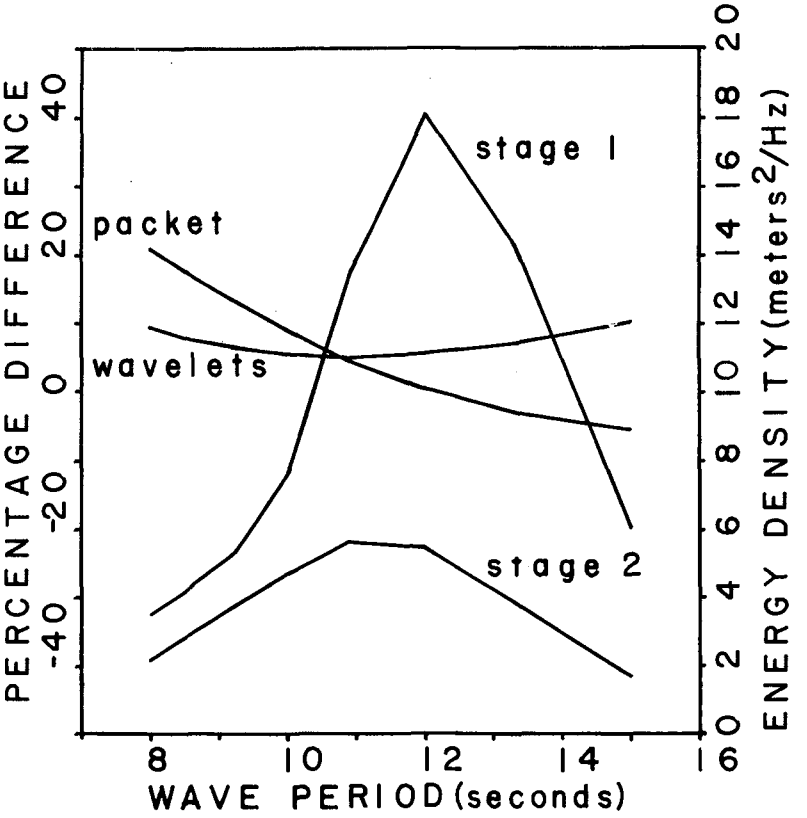

Figure 4. Comparison of Snell's law constants for wave packets and wavelets at Stage 1 and Stage 2 for Hurricane Betsy for measurement times of 1712-1743 and 1744-1815 UT on September 9, 1965. The percentage differences of the constants at Stage 2 from the corresponding values at Stage 1 are shown versus wave period. The energy density is presented for both stages for the time period 1712-1743 UT.

where x,y are the Cartesian coordinates, γ is the direction of the ray with respect to the positive x-axis, and s_v is the arc length along the ray. The ray curvature κ_G for the trajectory of a wave packet is given by

$$\kappa_G = \frac{d\theta}{ds_G} = \frac{1}{G}\left(\sin\theta\,\frac{\partial G}{\partial x} - \cos\theta\,\frac{\partial G}{\partial y}\right) \tag{11}$$

where θ is the direction of the packet ray with respect to the positive x-axis and s_G is the arc length along the ray.

3.1 Packet Ray Curvature

The derivation of the packet ray curvature is greatly simplified by using a x'y'-coordinate system which is chosen so that at each ray point the positive x'-axis is in the direction of the gradient of the water depth. As a result, the first partial derivatives of the water depth and the wave speeds with respect to y' vanish. From (2) the space derivative of G is then

$$\frac{\partial G}{\partial x'} = \frac{\partial U}{\partial x'}\cos\phi - U\sin\phi\left(\frac{\partial \theta'}{\partial x'} - \frac{\partial \gamma'}{\partial x'}\right) \tag{12}$$

Also

$$\partial\theta'/\partial x' = \left[(\partial G/\partial x')/G\right]\tan\theta' \tag{13}$$

$$\partial\gamma'/\partial x' = \left[(\partial v/\partial x')/v\right]\tan\gamma' \tag{14}$$

After (13), (14), and (12) are substituted into (11) and the result is simplified, the packet ray curvature is found to be

$$\kappa_G = \frac{\left[(\partial U/\partial x')/U\right] + \left[(\partial v/\partial x')/v\right]\tan\phi\,\tan\gamma'}{\csc\theta' + \tan\phi\,\sec\theta'} \tag{15}$$

This expression is used by Breeding (1978b) in a wave prediction program.

3.2 Properties of the Packet Ray Curvature

The ray curvature of a wave packet defined by (15) exhibits some very remarkable properties. To determine the important properties the discussion is simplified by taking the wave speed contours parallel to the y-axis. It is assumed that v, U, and their derivatives are continuous and finite. However, under various conditions the trigonometric terms of the equation can become infinite or have indeterminate forms. The value of κ_G approaches zero as the wave packet direction θ becomes either parallel or perpendicular to the wave speed contours, provided the wavelet direction γ is not parallel to the contours. This means that given a sufficiently long path, refraction tends to turn the wave packet so that it is directed either parallel or perpendicular to the wave speed contours. If θ is neither parallel nor perpendicular to the wave speed contours, then κ_G approaches infinity as γ becomes

parallel to the wave speed contours. In this case, due to the value of γ, the wave packet undergoes total reflection.

To determine the value of κ_G when there are indeterminate forms it is necessary to consider the variations of θ and γ as the indeterminate forms are approached. For example, (15) contains an indeterminate form when θ becomes perpendicular to the wave speed contours while γ becomes parallel to the contours. If γ approaches parallelism to the contours faster than θ approaches the perpendicular to the contours the value of κ_G becomes infinite.

The relationship between θ and γ due to refraction is clearly seen by integrating the ray curvature expressions (10) and (11). The y-derivatives being zero, integration of (11) leads to (4) which can be stated

$$(\sin \theta)/[U \cos (\theta - \gamma)] = C \tag{16}$$

which is Snell's law for a wave packet. Snell's law with phase velocity, which determines γ, is obtained by integrating (10). The cosine term in (16) can be replaced by the identity for the difference of two angles and the terms rearranged to yield

$$\tan \theta = (UC \cos \gamma)/(1 - UC \sin \gamma) \tag{17}$$

where the variation of θ appears only on the left side of the equation.

It is interesting to note that θ becomes zero if $\gamma = (2m+1)(\pi/2)$ where m is an integer. Thus if the wavelet direction becomes parallel to the wave speed contours the wave packet direction becomes perpendicular to the contours. Further, note that $\theta = (2m+1)(\pi/2)$ if $UC \sin \gamma = 1$. For this case the wave packet direction is parallel to the wave speed contours.

Snell's law can be used to derive an expression for $\cos (\theta - \gamma)$. Eq. (17) is substituted into the identity for $\tan (\theta - \gamma)$ and the result is simplified to obtain

$$\tan (\theta - \gamma) = (UC - \sin \gamma)/\cos \gamma \tag{18}$$

In terms of initial values, Snell's law with phase velocity can be written

$$\sin \gamma = v_r \sin \gamma_i \tag{19}$$

where $v_r = (v/v_i)$ and the subscript i denotes an initial value. Before refraction it is assumed that $\theta_i = \gamma_i$. Then

$$C = (\sin \gamma_i)/U_i \tag{20}$$

When (19) and (20) are substituted into (18), it is found that

$$\tan(\theta - \gamma) = \frac{(U_r - v_r)\sin\gamma_i}{(1 - v_r^2 \sin^2\gamma_i)^{\frac{1}{2}}} \tag{21}$$

where $U_r = (U/U_i)$. This result can be transformed by the use of an identity to

$$\cos(\theta - \gamma) = \left[1 + \frac{(U_r - v_r)^2 \sin^2\gamma_i}{1 - v_r^2 \sin^2\gamma_i}\right]^{-\frac{1}{2}} \tag{22}$$

Eqs. (1), (2), and (22) provide a useful means of computing the geometric group speed.

4 HYDRON EXAMPLES OF WAVE PACKET REFRACTION

To demonstrate the properties of wave packet refraction, examples of gravity water waves will be considered. Gravity water waves are particularly suited as examples because of their highly dispersive nature. The term 'hydron,' suggested by Purser and Synge (1962) and Synge (1962), will be used to denote the wave packet of water waves.

4.1 Waves Starting in Deep Water

In Figure 5 hydron trajectories are shown for waves beginning in deep water (water depth greater than one half the wavelength). The water depth contours are parallel. Initially $\theta_i = \gamma_i$ where each initial direction indicated on the figure is the angle between the hydron velocity vector and the normal to the depth contours. Regardless of the wave period, for deep water angles of incidence between 0^0 and 74.8^0 the hydrons follow paths such that the angles increase to the depth of the geometric group speed maximum (see Figure 7), then undergo a point of inflection, and then decrease shoreward. As a hydron approaches shore its direction becomes perpendicular to the wave speed contours and the packet ray curvature approaches zero. For deep water angles of incidence equal to or greater than 74.8^0 the hydron trajectories turn and move parallel to shore in water of intermediate depth. As the hydron direction becomes parallel to shore the packet ray curvature tends to vanish; this is apparent in ray number 5.

For comparison, monochromatic rays are shown in Figure 6 for the same conditions considered in Figure 5. For large incident angles there is a striking difference between hydron and monochromatic trajectories. Whereas all the hydron rays do not reach shore all the monochromatic rays do. Note that the wavelet direction at each point along a hydron path in Figure 5 is the same as the direction of the corresponding monochromatic ray at the corresponding water depth.

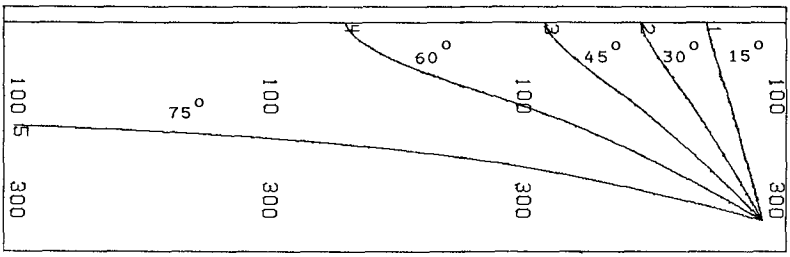

Figure 5. Hydron trajectories for a 20 s wave period for waves beginning in deep water. The water depth contours are parallel, the scale of the plot is 1 cm = 4.87 km, and the sounding depths are in meters. The initial hydron direction is shown for each ray and is the angle between the hydron velocity vector and the normal to the depth contours.

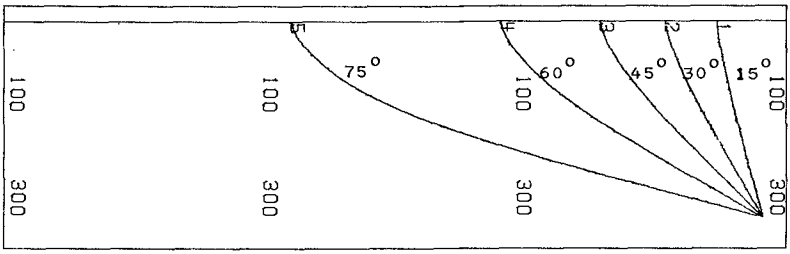

Figure 6. Monochromatic rays for comparison with the hydron rays in Figure 5.

It is interesting to compare the values of G and U when they differ due to refraction. As an example, for gravity water waves which begin in deep water it is found that

$$v_r = \tanh kh \tag{23}$$

$$U_r = \left(1 + \frac{2kh}{\sinh 2kh}\right) v_r \tag{24}$$

where h is the water depth. When (23) and (24) are substituted into (22) and the result is substituted into (2) it is found that

$$G = U \left[1 + \frac{(kh \sin \gamma_i \operatorname{sech}^2 kh)^2}{1 - (\sin \gamma_i \tanh kh)^2}\right]^{-\frac{1}{2}} \tag{25}$$

The ratio of the geometric group speed to its initial deep water value is presented for several incident angles in Figure 7. The initial hydron directions are defined as in Figure 5. The curve for $\gamma_i = 0^0$ is the same as obtained for the ratio of U to the value of U in deep water. The amount by which the other curves differ from it is a measure of the difference between G and U.

Inspection of Figure 7 shows for a given γ_i that the maximum of G/G_i occurs at a greater value of kh than does the minimum of G/U. An increase in γ_i causes a shift in both the minimum of G/U and the maximum of G/G_i to larger values of kh. Further, the maximum peak tends to get flattened out. The curve for $\gamma_i = 74.8^0$ is seen to stop abruptly at the maximum value of G/G_i.

When $\gamma_i = 30^0$ the maximum percentage difference of G from U is 2.70%. When $\gamma_i = 45^0$ the value is 5.91%, for $\gamma_i = 60^0$ it is 10.03%, and for $\gamma_i = 74.79^0$ the value is 14.27%.

4.2 Reflection Points

To obtain a reflection point is is necessary that the waves propagate into deeper water and that the initial direction of the hydron ($\theta_i = \gamma_i$) exceed a critical angle. The reflection point occurs at an intermediate water depth when, through refraction, the wavelets are turned parallel to the wave speed contours.

In Figure 8 two rays are shown in which the wave period is 20 sec and the initial water depth is 15 m. For this case a reflection point occurs if $\theta_i \geq 22.2^0$. Ray number 1 reaches deep water since $\theta_i = 15^0$. For ray number 2, $\theta_i = 23^0$, and a reflection point occurs at a water depth of 200 m. The variation of the hydron and wavelet directions with water depth for this ray are shown in Figure 9. The wavelet angle increases continuously with water depth and becomes parallel to the water depth contours at the reflection point. The hydron angle first increases, goes through a maximum, and then becomes perpendicular to

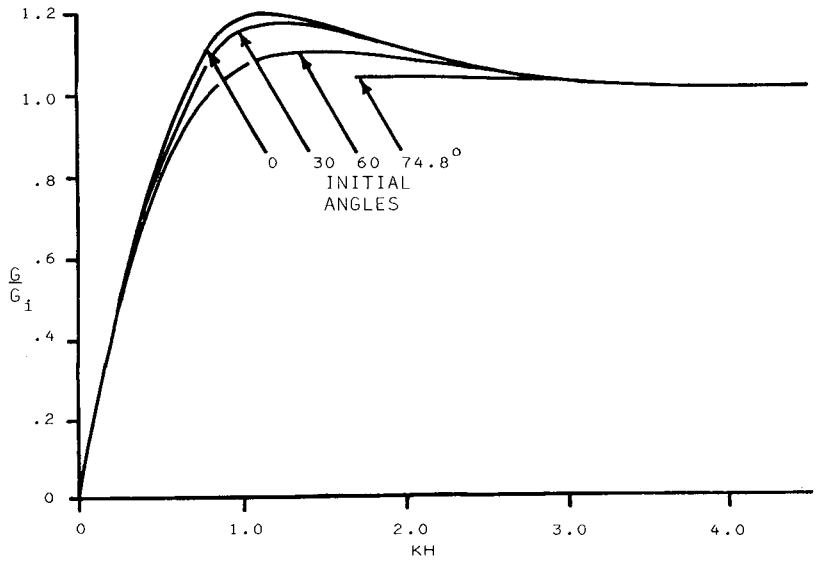

Figure 7. The variation of the geometric group speed with kh for hydrons beginning in deep water. The initial value of the geometric group speed is G_i. The hydron directions are defined as in Figure 5.

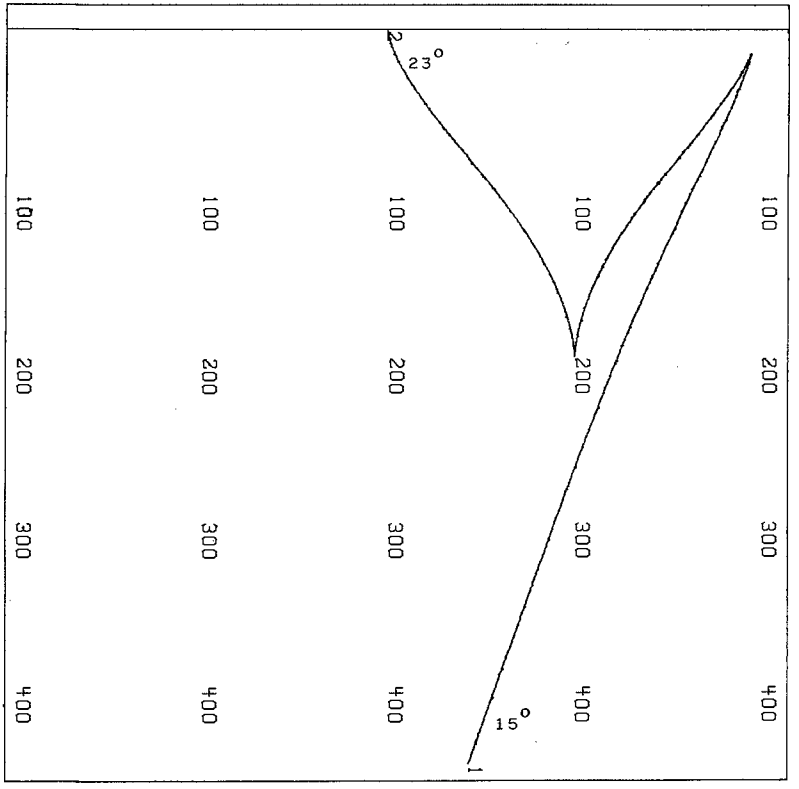

Figure 8. Hydron trajectories for a 20 s wave period for waves which begin at an intermediate water depth. The scale of the plot is 1 cm = 3.10 km and the sounding depths are in meters. The initial hydron direction is shown for each ray and is defined as in Figure 5.

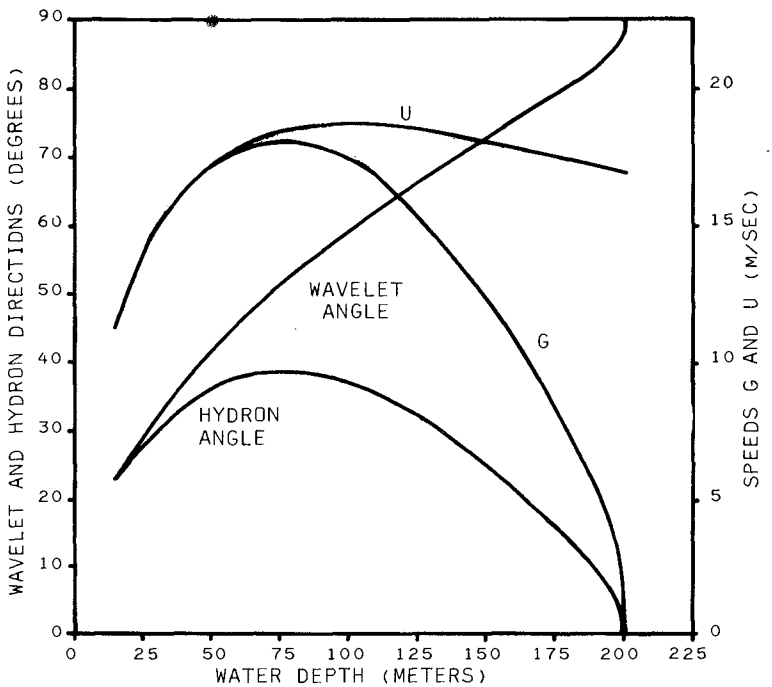

Figure 9. Variations of the wavelet direction γ, hydron direction θ, the speed $U = d\omega/dk$, and the geometric group speed $G = U \cos(\theta-\gamma)$ up to the reflection point for ray number 2 in Figure 8.

the water depth contours at the reflection point. This is clearly seen in Figure 8.

Plots of how G and U vary with water depth in approaching the reflection point are shown in Figure 9. Both speeds have a maximum value. However, there is a marked contrast between G and U at the reflection point where the geometric group speed is zero.

In Figure 10 the ratio of the packet ray curvature to its initial value is sketched as a function of the wavelet direction for ray number 2 in Figure 8. The most striking feature of this curve is that within about 2^0 of the reflection point the packet ray curvature suddenly goes to infinity.

It is interesting to observe that the velocity of the wave packet goes to zero at the reflection point. This is exactly what the velocity of a particle should do when there is reflection. Therefore, in water waves, as in quantum mechanics, the wave-particle duality is encountered.

5 CONCLUSIONS

Directional gravity water wave data obtained simultaneously at two field stations were used to test the refraction laws for the wave packets (hydrons) and wavelets. It is found that the constancy of Snell's laws is established with equal precision for both the wave packets and wavelets. From the results it is concluded that the wave packets refract according to Snell's law with the geometric group velocity while the wavelets within a packet refract according to Snell's law with phase velocity.

Refraction causes a hydron trajectory to become directed either parallel or perpendicular to the water depth contours. In either case the packet ray curvature will vanish. For hydrons propagating toward deep water, if the initial direction exceeds a critical angle total reflection occurs. At the reflection point the wavelet direction becomes parallel to the wave speed contours, the hydron direction becomes perpendicular to the contours, the geometric group velocity goes to zero, and the packet ray curvature becomes infinite.

6 ACKNOWLEDGMENTS

The data were collected and the spectral analysis obtained at the Naval Coastal Systems Center, Panama City, Florida, by George B. Austin and Carl M. Bennett, respectively. I thank them for their cooperation and suggestions.

Further, I thank Franklyn C. W. Olson, Kenneth C. Matson, and Kimberly Crane Oppenheimer for their help in preparing this paper. The research was supported by the Geography Programs, Earth Sciences Division, Office of Naval Research (USA) under Contract No. N00014-77-C-0329.

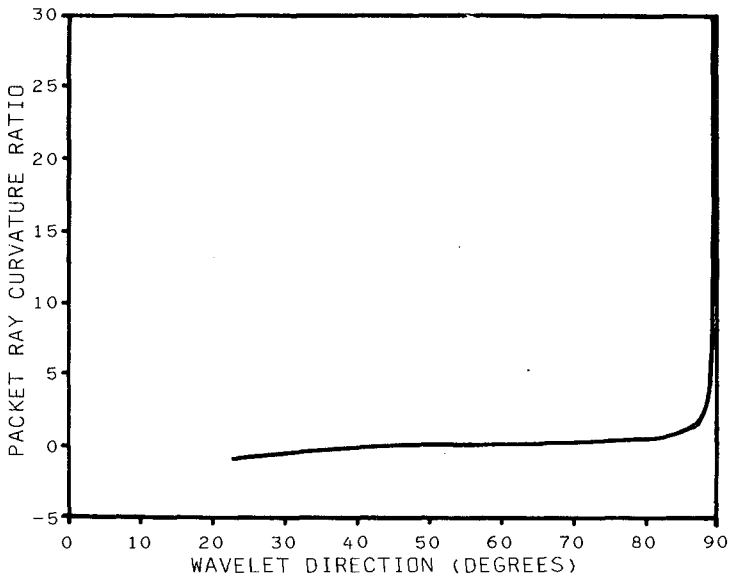

Figure 10. The ratio of the hydron ray curvature to its absolute initial value as a function of the wavelet direction up to the reflection point for ray number 2 in Figure 8.

7 REFERENCES

Arthur, R.S., Munk, W.H., and Isaacs, J.D. (1952). The direct construction of wave rays. Trans. Am. Geophy. Union, Vol. 33, No. 6, pp. 855-865.

Bennett, C.M. (1972). The directional analysis of ocean waves: an introductory discussion, 2nd ed. Naval Coastal Systems Center Report No. 144-72. Unpublished.

Black, J.L. (1979). Hurricane Eloise directional wave energy spectra. Proc. 11th Annual Offshore Tech. Conf., Houston, paper OTC 3594.

Breeding, J.E., Jr. (1972). Refraction of gravity water waves. Thesis (Ph.D.), Columbia Univ.

Breeding, J.E., Jr., (1978a). Velocities and refraction laws of wave groups: a verification. J. Geophys. Res., Vol. 83, No. C6, pp. 2970-2976.

Breeding, J.E., Jr. (1978b). A method for calculating wave packet trajectories and wave heights: part 2. Dep. of Oceanogr., Florida State Univ. Report No. JEB-4. Unpublished.

Munk, W.H. and Arthur, R.S. (1952). Wave intensity along a refracted ray. Gravity waves, National Bureau of Standards Circular 521. pp. 95-108.

Munk, W.H., Miller, G.R., Snodgrass, F.E., and Barber, N.F. (1963). Directional recording of swell from distant storms. Phil. Trans. Roy. Soc. London, Ser. A, Vol. 255, No. 1062, pp. 505-584.

Purser, W.F.C. and Synge, J.L. (1962). Water waves and Hamilton's method. Nature, Vol. 194, No. 4825, p. 268.

Synge, J.L. (1962). Water waves and hydrons. Science, Vol. 138, No. 3536, pp. 13-15.